

Two-dimensional algorithm of the density-matrix renormalization group

Tao Xiang, Jizhong Lou, and Zhaobin Su

Institute of Theoretical Physics, Academia Sinica, P.O. Box 2735, Beijing 100080, The People's Republic of China

(Received 20 February 2001; revised manuscript received 25 April 2001; published 21 August 2001)

We propose an approach to implement the density-matrix renormalization group (DMRG) in two dimensions. With this approach the initial blocks of a $L \times L$ lattice are built up directly from the matrix elements of a $(L-1) \times (L-1)$ lattice and the topological characteristics of two-dimensional lattices are preserved in the iteration of DMRG. By applying it to the spin-1/2 Heisenberg model on both square and triangular lattices, we find that this approach is significantly more efficient and accurate than other two-dimensional DMRG methods currently in use.

DOI: 10.1103/PhysRevB.64.104414

PACS number(s): 71.27.+a, 75.10.-b

I. INTRODUCTION

The density matrix renormalization group (DMRG) is an optimized iterative numerical method. Since its development by White in 1992,¹ this method has achieved tremendous success in studying ground state properties of one-dimensional (1D) interacting electrons. It has also been successfully extended to finite temperatures,^{2,3} to momentum space,⁴ and to the calculation of dynamic correlation functions.⁵⁻⁷

The DMRG starts from a small system which can be handled rigorously. A large chain, called a superblock, is then built up from this small system by adding a number of sites at a time. At each stage, the superblock consists of system and environment blocks in addition to a number of extra sites. Graphically, a superblock can be represented as $(S \bullet_s \bullet_e E)$, where S and E represent the system and environment blocks and \bullet_s and \bullet_e the extra sites added to S and E , respectively. S and \bullet_s (similarly E and \bullet_e) form an augmented block, which becomes the system (environment) block in the next iteration. However, in order to keep the size of the superblock basis from growing, the basis for the augmented blocks is truncated. Hence the DMRG is a basis truncation method. However, unlike the conventional renormalization group method, the truncation is done for each augmented subblock and the basis states retained are determined not by their energies but by their probabilities projecting onto the ground state (or other targeted states) of the superblock. These probabilities are determined by the reduced density matrix of the augmented system (or environment) block.

To construct the density matrix, the ground state $|\psi\rangle$ of the superblock is first diagonalized with the Lanczos or other sparse matrix diagonalization algorithm. The reduced density matrix of the augmented system (or environment) is defined by tracing out from $|\psi\rangle\langle\psi|$ all the degrees of freedom that do not belong to this block:

$$\rho = \text{Tr}_{(E \oplus \bullet_e)} |\psi\rangle\langle\psi|. \quad (1)$$

Thus $(E \oplus \bullet_e)$ is considered as a statistical bath to the augmented system. The density matrix is semipositive definite.

Its eigenvalue is equal to the projection probability of the corresponding eigenvector in $|\psi\rangle$, i.e.,

$$\lambda_l = \sum_j |\langle\lambda_l, e_j | \psi\rangle|^2, \quad (2)$$

where $(\lambda_l, |\lambda_l\rangle)$ is an eigenpair of ρ and $\{|e_j\rangle\}$ is a basis set of $(E \oplus \bullet_e)$.

Given the density matrix, an entropy can be defined for the augmented system according to the standard thermodynamic relation

$$S = -\text{Tr} \rho \ln \rho = -\sum_l \lambda_l \ln \lambda_l. \quad (3)$$

The maximum of the function $f(\lambda) \equiv -\lambda \ln \lambda$ is located at $\lambda = e^{-1}$. When $0 \leq \lambda < e^{-1}$, $f(\lambda)$ increases monotonically with λ . When $\lambda > e^{-1}$, $f(\lambda)$ decreases with λ . No more than two λ_l can be larger than e^{-1} since $\sum_l \lambda_l = 1$. Thus if the contribution to the entropy from the largest λ_l is larger than that from the largest discarded eigenvalue of ρ , the DMRG is also a maximum entropy method.

There are two approaches in forming a superblock. In the literature they are often referred to as the finite and infinite lattice approaches. In the infinite lattice approach in one dimension, the environment block is generally chosen as the space reflection of the system. In the finite lattice approach, the size of the superblock is fixed and the environment block is chosen as the remaining part of the lattice for a given system block. The infinite lattice approach allows the size of the superblock to be flexible and can be used to study the thermodynamic limit directly. However, the finite size approach is more accurate in calculating quantities for a system with fixed lattice size.

The DMRG can also be used to study thermodynamic properties of a 1D quantum³ or 2D classical system.² In this case, the transfer matrix of a Hamiltonian system, instead of the Hamiltonian itself, is diagonalized. The free energy and other thermodynamic quantities are determined by the maximum eigenvalue of the transfer matrix. The transfer-matrix DMRG method treats directly an infinite lattice system and has therefore no finite lattice size effect.

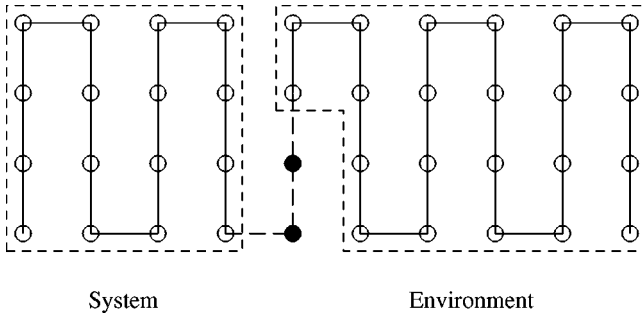


FIG. 1. A superblock in a “multichain” algorithm. The system and environment blocks are enclosed by dashed lines. Black spots are the sites added to the system and environment.

A simple extension of the DMRG to more than 1D would be to replace the single sites added between the blocks with a row of sites, either along a principal axis⁸ or along a diagonal.⁹ However, the extra degrees of freedom added to the system would make the size of the Hilbert space prohibitively large. Therefore, the two-dimensional algorithm should be developed so that only a single site is added to each subblock at a time.

In practice the extension of the DMRG to more than 1D is to map a higher dimensional lattice onto a 1D one, namely, to choose a path to order all lattice sites.¹⁰ The mapping breaks the lattice symmetry and introduces long range interactions among lattice sites. Therefore, the 2D procedure differs from the 1D one in that there are additional connections between the system and environment blocks.

A typical mapping, as illustrated in Fig. 1, is to fold a 1D zipper into 2D. This is basically a multichain approach since the length of the folded zipper is unlimited but the width is fixed. For a 2D gas of noninteracting electrons, Liang and Pang found that the number of states needed to maintain a certain accuracy grows exponentially with the width of the lattice.¹⁰ This convergence was also confirmed for an algorithm where a row of sites was added at each step.⁸ Although no proof has been given, this statement is often referred to as most probably valid for any 2D DMRG calculation.

This multichain approach is simple to implement in the DMRG iteration. However, with this approach, the calculations on $(L-1) \times (L-1)$ and $L \times L$ are performed independently. The information obtained from the iterations on a $(L-1) \times (L-1)$ lattice is not used in the preparation of the initial sub-block matrices in the calculation for a $L \times L$ lattice. This is undoubtedly a loss of the efficiency. It may result in the loss of the accuracy as well, since the topological characteristics of square lattices are not well manifested in the preparation of the initial block states and the sweeping procedure of DMRG iterations.

The momentum space DMRG provides an alternative way to implement the DMRG in two or higher dimensions.⁴ In this representation the momentum is conserved. This leads to a strong restriction on the basis states and allows the number of states kept to increase substantially. Unlike its real space counterpart, the momentum space DMRG treats the kinetic energy rigorously. Hence this method works better in the weak coupling limit. However, the application of the mo-

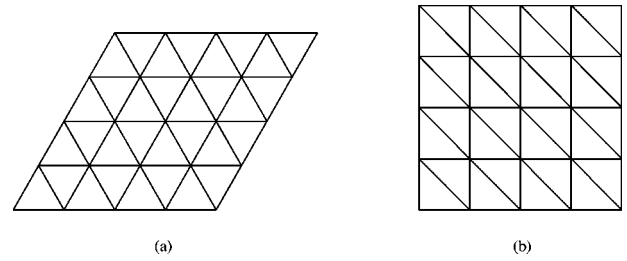


FIG. 2. A $L \times L$ ($L=5$ here) triangular lattice (a) can be taken as a $L \times L$ square lattice with extra next-nearest-neighbor coupling (b).

mentum space DMRG has its own limitations. For example, it is very difficult, if not completely impossible, to apply this method to a pure spin system such as the Heisenberg model.

In this paper, we introduce an approach to implement the DMRG in real space in 2D. Instead of ordering the lattice sites row by row as in the multichain approach, we order the lattice sites by the order along the diagonal direction. This allows us to build up the initial system and environment of a $L \times L$ lattice system based on the results on a $(L-1) \times (L-1)$ lattice and is particularly suitable for handling 2D lattice models.

The rest of the paper is arranged as the following. In Sec. II a diagonally ordered algorithm of the 2D DMRG is introduced. In Sec. III, as an example of the application of the algorithm, the ground state energy of the spin-1/2 Heisenberg model is evaluated on both square and triangular lattices. The study is summarized in Sec. IV.

II. A 2D ALGORITHM OF THE DMRG

In this section we will take the square lattice as an example to show how to build up initial blocks of a $L \times L$ lattice from a $(L-1) \times (L-1)$ lattice. The extension to any 2D lattice which can be topologically transformed to a square lattice by adding or removing some of the nearest or next nearest neighbor interactions from the square lattice, such as triangular, hexagonal, and Kagomi lattices (an example for such a transformation is given in Fig. 2), is straightforward.

Let us start from a 2×2 lattice. Figure 3(a) shows the order of the sites after the $2D \rightarrow 1D$ mapping. As the system is small, the Hamiltonian can be fully diagonalized.

Figure 3(b) shows the configuration of the initial superblock for a 3×3 lattice system. As indicated by the number shown in the figure, the lattice sites are ordered from the lower left corner to the upper right corner along the diagonal. The initial system contains three sites linked by the solid line in the lower left corner. The initial environment contains all the four sites in the upper right 2×2 lattice. All the matrix elements for these initial sub-blocks can be obtained from the results previously obtained on the 2×2 lattice. We add site 4 to the system and site 6 to the environment to form the augmented system and environment blocks. Unlike in a real 1D system, these two added sites are not nearest neighbors in the mapped 1D system. After a standard DMRG calculation for this superblock, the augmented system block can be updated and taken as the new system in the next iteration.

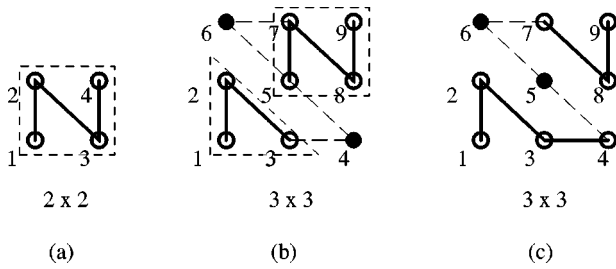


FIG. 3. (a) A 2×2 lattice. (b) The initial configuration of superblock for a 3×3 lattice system. As indicated by the numbers, the lattice sites are ordered along the diagonal direction. The initial system contains three sites linked by the solid line in the lower left corner. The initial environment contains four sites, also linked by the solid line, at the upper right corner. (c) Same as for (b) but for the next iteration. Black spots are the extra sites added into the superblock.

In the next iteration [Fig. 3(c)] the system contains four sites (i.e., sites 1–4) and the environment contains only three sites at the upper right corner (i.e., sites 7–9). Since the two sites (i.e., sites 5 and 6) to be added to the system and environment are nearest neighbors in the mapped 1D lattice, from now on the DMRG finite system sweeping can be done exactly as in a true 1D system.

Similarly, the DMRG iterations on a 4×4 lattice can be done based on the results of the 3×3 lattice. As for a 3×3 lattice, a 4×4 lattice [Fig. 4(a)] can be formed by two corner cut off 3×3 lattices with two isolated sites. The initial system contains 6 sites linked by a solid line in the lower left corner (i.e., sites 1–6) and the initial environment contains 8 sites, also linked by a solid line, in the upper right 3×3 lattice (i.e., sites 8,9,11–16). The configurations of these two blocks can be found from the previously studied 3×3 lattice with or without a space reflection. We add site 7 to the system and site 10 to the environment to form the augmented system and environment blocks. Again, these two sites are not nearest neighbors in the mapped 1D system. But

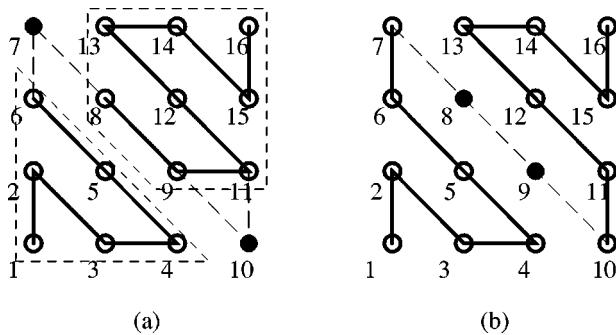


FIG. 4. (a) A 4×4 lattice decomposed as two partially overlapped 3×3 lattices (enclosed by the short dashed squares) and two sites at the two corners outside these 3×3 lattices (i.e., sites 6 and 10). The number besides each lattice site gives the order in the mapped 1D system. The sites in a system or environment block are linked by solid lines. Black spots are the sites added in. (b) Same as for (a) but for the next iteration. The environment (sites 10–16) is a space reflection of the system (sites 1–7) with respect to the center of the 4×4 lattice.

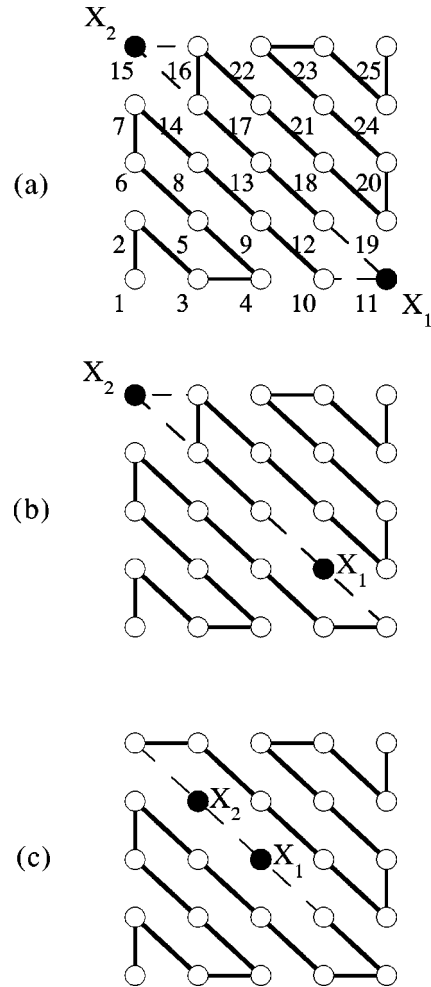


FIG. 5. The first three initial configurations of superblocks for a 5×5 lattice system. At the first two iterations (a) and (b) the two sites which are added to the system and environment (i.e. X_1 and X_2) are not next to each other in the mapped 1D system. At the third iteration (c) X_1 and X_2 become next to each other in the mapped 1D system.

the standard DMRG calculation can be done as usual. The augmented system block is then updated and taken as the new system in the next iteration.

In the next iteration [Fig. 4(b)], the augmented system in the last iteration becomes the new system. It contains seven sites (i.e., sites 1–7). In this case, since the total number of sites in the environment is also seven, the environment can therefore be taken as the space reflection of the system with respect to the center of the 4×4 lattice, i.e., sites 10–16. All the matrix elements of this environment can be obtained from the space reflection of the system. The sites now added into the system and environment are the two nearest neighboring sites in the mapped 1D system. Thus starting from this iteration, the standard finite system sweeping can be done as in a 1D system, without considering how the 4×4 lattice is constructed from the 3×3 lattices.

The above procedure can be repeated to larger square lattices. In general, the initial superblocks of a $L \times L$ lattice can be formed based on the results of the system and environment blocks in a $(L-1) \times (L-1)$ lattice. We order all the

TABLE I. Comparison of the ground state energy per bond of the Heisenberg model on square and triangular lattices with free boundary conditions obtained by our approach E_{2d} with that obtained by the multichain approach E_{mc} . m is the number of states retained. The lattice size is L^2 .

L	Square lattice			Triangular lattice		
	E_{2d}	E_{mc}	$(E_{mc}-E_{2d})/ E_{mc} $	E_{2d}	E_{mc}	$(E_{mc}-E_{2d})/ E_{mc} $
$m=50$						
6	-0.361972	-0.361919	1.5×10^{-4}	-0.210692	-0.210732	-1.9×10^{-4}
8	-0.35204	-0.351149	2.6×10^{-3}	-0.199179	-0.198752	2.1×10^{-3}
10	-0.344292	-0.341389	8.4×10^{-3}	-0.192918	-0.189763	1.6×10^{-2}
12	-0.337374	-0.332574	1.4×10^{-2}	-0.187242	-0.182806	2.4×10^{-2}
$m=100$						
6	-0.362096	-0.362089	1.9×10^{-5}	-0.211171	-0.211196	-1.2×10^{-4}
8	-0.353213	-0.353057	4.3×10^{-4}	-0.200426	-0.200494	-3.3×10^{-4}
10	-0.347043	-0.345771	1.3×10^{-3}	-0.195015	-0.192714	1.2×10^{-2}
12	-0.341588	-0.338833	8×10^{-3}	-0.189992	-0.186441	1.9×10^{-2}

lattice sites similar to a folded zipper with unequal width along the diagonal. If the first site at the lower left corner of the $L \times L$ lattice is labeled as 1, then the two sites to be added in will have the coordinates $X_1 = (L-1)L/2 + 1$ and $X_2 = L(L+1)/2$ in the mapped 1D system, respectively. (An example is given in Fig. 5 for a 5×5 lattice system.) We take the first $(L-1)L/2$ sites in the lower left corner as the initial system and all the sites in the upper right $(L-1) \times (L-1)$ square lattice not used by the system as the initial environment. The DMRG calculation can be done as before. The system is always augmented and updated. At the first few iterations, the site which is added to the environment is fixed at X_2 and is not exactly next to X_1 in the mapped 1D lattice. This continues until the environment can be generated by the center reflection of the system and the two sites added to these two blocks become nearest neighbors in the mapped 1D system. After that the standard finite system sweeping can be done as in an ordinary 1D lattice.

III. THE 2D HEISENBERG MODEL

In this section, we take the spin-1/2 Heisenberg model as an example to demonstrate how good our approach is compared with the multichain approach. The ground state energies on both square and triangular lattices are evaluated. For these 2D systems, there are currently rather precise results available, mainly from large-scale Monte Carlo calculations and series expansions. Therefore the accuracy of our results can be assessed by comparing with these results.

The Heisenberg model is defined by the Hamiltonian

$$H = \sum_{\langle ij \rangle} \mathbf{S}_i \cdot \mathbf{S}_j, \quad (4)$$

where \mathbf{S}_i is the spin operator and the summation runs over all nearest neighbors. In real space at the same parameters and number of states, the truncation error in a system with periodic boundary conditions is usually much higher than with free boundary conditions, therefore we use free boundary conditions.

The total spin \mathbf{S}^2 is a good quantum number for the isotropic Heisenberg model. This symmetry has been used in obtaining all the results presented below. We have also performed finite system iterations using both our algorithm and the multichain one. In the multichain calculations, we have used an algorithm introduced in Ref. 11 to build up the initial system or environment blocks.

Table I compares the ground state energy per bond obtained by our approach E_{2d} with that obtained by the multichain approach E_{mc} on both square and triangular lattices. For square lattices, E_{2d} is always lower than E_{mc} . Since the DMRG satisfies the variational principle, this means that the results obtained with our approach are more accurate than the multichain ones. Moreover, the difference $(E_{mc} - E_{2d})/|E_{mc}|$ increases with increasing lattice. Thus the improvement of our approach over the multichain approach becomes more and more significant as the lattice size is increased. For triangular lattices, E_{2d} is slightly higher than E_{mc} when L is small. However, for large lattices E_{2d} is much

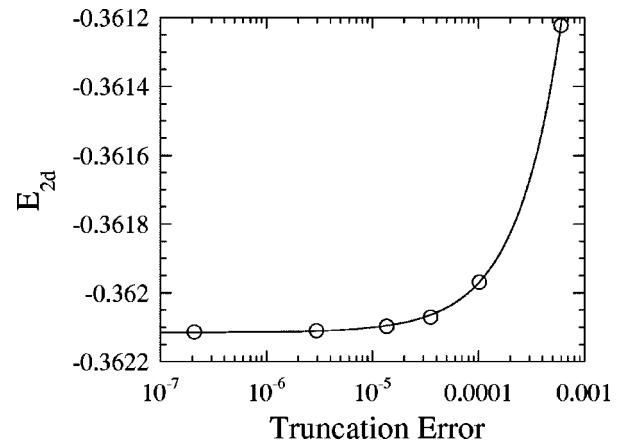


FIG. 6. The ground state energy per bond E_{2d} as a function of the truncation error for the spin-1/2 Heisenberg model on a 6×6 square lattice with free boundary conditions. The solid line is a polynomial fit to the data.

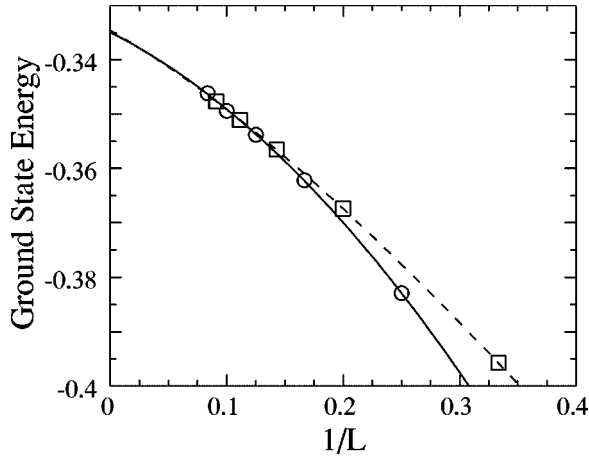


FIG. 7. Ground state energy E_{2d} versus $1/L$ of the Heisenberg model with free boundary conditions on square lattices. The behavior of E_{2d} on even lattices is different to that on odd lattices. But the extrapolated value in the limit $1/L \rightarrow 0$ is the same within numerical errors.

more accurate than E_{mc} . The increase of $(E_{mc} - E_{2d})/|E_{mc}|$ with increasing size in the triangular lattice is even larger than in the square one.

For a given L , an accurate estimate of the ground state energy (similarly other physical quantities) can be obtained by extrapolating E_{2d} to the limit $m \rightarrow \infty$. This can also be done¹² by extrapolating E_{2d} with respect to the truncation error $\Delta\varepsilon$, since the limit $m \rightarrow \infty$ is equivalent to the limit $\Delta\varepsilon \rightarrow 0$. The extrapolation with respect to the number of retained states is difficult to implement since the asymptotic behavior of E_{2d} in the limit $m \rightarrow \infty$ is unknown and there is some uncertainty in determining the function used in the extrapolation. However, we find that the $\Delta\varepsilon$ dependence of E_{2d} is generally very simple and can be well described by a power law in the limit $\Delta\varepsilon \rightarrow 0$. An example is given in Fig. 6 where the $\Delta\varepsilon$ dependence of E_{2d} on a 6×6 square lattice is shown. In the figure, the solid line is a polynomial fit (up to the quadratic term in $\Delta\varepsilon$) to the data. From the fit the ground state energy per bond for this 6×6 system is estimated to be -0.36212 . For other cases, this fitting procedure can be similarly done.

To obtain the ground state energy in the thermodynamic limit, we need to do a finite size scaling for the results obtained from the above extrapolation. In a periodic system, the leading size correction to the ground state energy per bond is of order $1/L^3$.¹³ However, in an open system as considered here, the finite size effect is stronger and the leading size correction is of order $1/L$.

Figures 7 and 8 show the scaling behavior of the ground state energy on square and triangular lattices, respectively. For the square lattice, the extrapolated ground state energy in the limit $1/L \rightarrow 0$ is $E_\infty \approx -0.3346$. This agrees very well with the probably best currently available estimate, obtained from large-scale quantum Monte Carlo calculations of $E_\infty \approx -0.334719(3)$.¹⁴ The result of spin wave theory is $E_\infty = -0.33475$ up to the fourth order correction.¹⁵ For the triangular lattice, the extrapolated result is $E_\infty \approx -0.1814$. It is

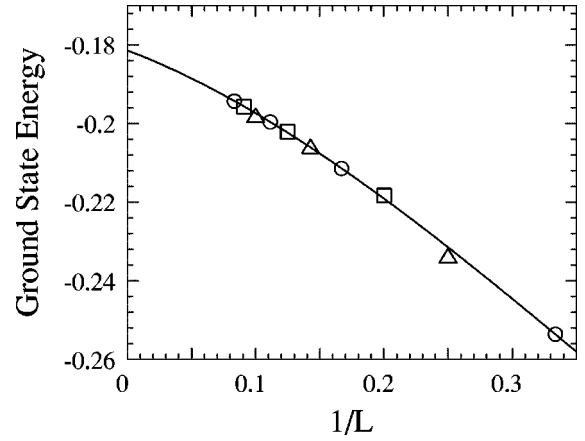


FIG. 8. E_{2d} versus $1/L$ for the Heisenberg model with free boundary conditions on triangle lattices. The solid line is a polynomial fit to the data with $\text{mod}(L,3)=0$.

also consistent with the quantum Monte Carlo results obtained by Capriotti *et al.*,¹⁶ $E_\infty \approx -0.1819$, and by Bernu *et al.*,¹⁷ $E_\infty \approx -0.1825$. The second order spin wave result is $E_\infty = -0.1822$.¹⁸

The above comparison indicates that accurate results for the ground state energy can be obtained using the algorithm introduced above. In obtaining these results, the symmetry of the total spin S^2 is considered and up to 300 states are retained. This calculation can be readily done on a moderate workstation. With the aid of modern parallel computers, we should be able to keep more states (e.g., 3000 states) and to further increase the accuracy.

IV. CONCLUSION

We have developed an approach to implement the real space DMRG in 2D. We point out that a $L \times L$ lattice can be taken as an assembly of two partially overlapped $(L-1) \times (L-1)$ lattices plus two extra sites and therefore the initial blocks of a $L \times L$ system can be built up directly from the blocks of a $(L-1) \times (L-1)$ system. This preserves a higher degree of the symmetry of 2D lattice than in the multichain approach and can be readily used in the DMRG calculation. For the spin-1/2 Heisenberg model on both square and triangular lattices, the ground state energies obtained with this approach are consistent with the quantum Monte Carlo results and better than those obtained with the multichain approach for large lattice systems.

ACKNOWLEDGMENTS

T.X. acknowledges the hospitality of the Interdisciplinary Research Center in Superconductivity of the University of Cambridge, where part of the work was done, and the financial support from the National Natural Science Foundation of China and from the special funds for Major State Basic Research Projects of China.

- ¹S. R. White, Phys. Rev. Lett. **69**, 2863 (1992).
²T. Nishino, J. Phys. Soc. Jpn. **64**, L3598 (1995).
³R. J. Bursill, T. Xiang, and G. A. Gehring, J. Phys.: Condens. Matter **8**, L583 (1996); X. Wang and T. Xiang, Phys. Rev. B **56**, 5061 (1997); T. Xiang, *ibid.* **58**, 9142 (1998); T. Xiang and X. Wang, in *Lecture Note in Physics*, edited by I. Peschel *et al.* (Springer, Berlin 1999), Chap. 5; N. Shibata, J. Phys. Soc. Jpn. **66**, 2221 (1997).
⁴T. Xiang, Phys. Rev. B **53**, 10 445 (1996).
⁵K. A. Hallberg, Phys. Rev. B **52**, 9827 (1995).
⁶Y. Anusooya, S. Pati, and S. Ramasesha, J. Chem. Phys. **106**, 1 (1997).
⁷T. D. Kühner and S. R. White, Phys. Rev. B **60**, 335 (1999).
⁸M. S. L. du Croo de Jongh and J. M. J. van Leeuwen, Phys. Rev. B **57**, 8494 (1998); M. S. L. du Croo de Jongh, Ph.D. thesis, Leiden University, 1999.
⁹P. Henelius, Phys. Rev. B **60**, 9561 (1999).
¹⁰S. D. Liang and H. B. Pang, Phys. Rev. B **49**, 9214 (1994).
¹¹R. M. Noack, S. R. White, and D. J. Scalapino, in *Computer Simulations in Condensed Matter Physics VII*, edited by D.P. Landau, K.K. Mon, and H.B. Schüttler (Spinger Verlag, Heidelberg, 1994).
¹²E. Jeckelmann and S. R. White, Phys. Rev. B **57**, 6376 (1998).
¹³T. Einarsson and H. J. Schulz, Phys. Rev. B **51**, 6151 (1995).
¹⁴A. W. Sandvik, Phys. Rev. B **56**, 11 678 (1997), and references therein.
¹⁵W. Zheng and C. J. Hamer, Phys. Rev. B **47**, 7961 (1993).
¹⁶L. Capriotti, A. E. Trumper, and S. Sorella, Phys. Rev. Lett. **82**, 3899 (1999).
¹⁷B. Bernu, C. Lhuillier, and L. Pierre, Phys. Rev. Lett. **69**, 2590 (1992).
¹⁸S. J. Miyake, J. Phys. Soc. Jpn. **61**, 983 (1992).